Green Chemistry

Cite this: *Green Chem.*, 2011, **13**, 272

www.rsc.org/greenchem

COMMUNICATION

# A flexible one-pot route to metal/metal oxide nanocomposites†

**Zoë Schnepp, Simon R. Hall, Martin J. Hollamby and Stephen Mann***

***Received 19th July 2010, Accepted 1st December 2010***
**DOI: 10.1039/c0gc00338g**



**We report a one-pot route to Au/$CeO_2$ nanocomposites. A readily-available biopolymer, sodium alginate, is exploited for controlled formation and stabilisation of gold nanoparticles followed by *in situ* growth of a sponge-like network of $CeO_2$ nanoparticles. The flexible nature of this method as a general route to mixed metal/metal oxide nanocomposites is also demonstrated.**

## Introduction

A key area of focus in current materials synthesis is the formation of nano-structured composites of two or more materials. In this way, it is possible to combine the properties of the individual components, or even generate entirely new effects through surface interactions. Of particular interest are composites of metal nanoparticles with a metal oxide support.[1–3] These have shown promise in a wide range of applications, including medical imaging, sensors and catalysis. However, current routes to metal/metal oxide nanocomposites are typically multi-step, involving pre-fabrication of the metal oxide support *via e.g.* sol–gel,[4] microemulsion[5] or hydrothermal[6] syntheses. These supports often require numerous washing cycles to remove solvent or surfactant, before the introduction of metal nanoparticles as a separate step. As such, a one-pot route to metal/metal oxide nanocomposites would have clear, considerable advantages.

Recently, biopolymers have been shown to exert a remarkable degree of control over the nucleation and growth of crystalline metal oxides.[7] Many biopolymers contain metal-binding functional groups which can be used to pre-organize aqueous metal cations within a gel structure. Alginate, for example, is the structural biopolymer found in seaweed and contains blocks of guluronate monomers (Fig. 1a) that are readily crosslinked by strong electrostatic bonds to multivalent metal cations. In this way, the polymer forms an extended gel network in water, with metal cations dispersed throughout the structure. Another characteristic of many biopolymers is their high thermal stability.[8,9] As a result, they are able to maintain the pre-organized dispersion of metal cations to relatively high temperatures. In solid state synthesis, this means that they can influence the nucleation and growth of crystalline phases. This has already been demonstrated in the formation of nanowires and nanoparticles of several metal oxides.

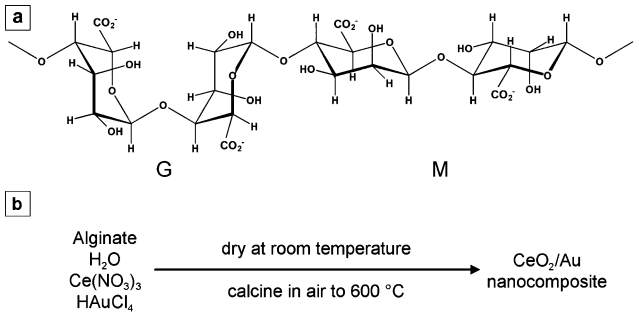


**Fig. 1** (a) Structure of alginate showing guluronate (G) and mannuronate (M) epimers, and (b) schematic showing the synthesis procedure for Au/$CeO_2$ nanocomposites.

In this paper, we couple the metal binding and structure-directing capacity of the biopolymer alginate with its ability to reduce precious metal salts to nanoparticles. In this way, we have developed a simple, one-pot route to metal/metal oxide nanocomposites. The concept is demonstrated in the synthesis of an Au/$CeO_2$ nanocomposite (Fig. 1b). Au supported on $CeO_2$ is widely studied, particularly in the field of oxidation catalysis,[10,11] but to the best of our knowledge this is the first example of the formation of such a system *via* a one-pot process. In this synthesis, the biopolymer first reduces aqueous $Au^{3+}$ and stabilises the resulting nanoparticles. On heating, the pre-organization of $Ce^{3+}$ cations within the polymer gel leads to constrained nucleation of $CeO_2$ nanoparticles. Finally, the decomposition products of the biopolymer restrict sintering of the Au and $CeO_2$ nanoparticles before the final transformation to the composite product. The flexibility and general nature of this method is then demonstrated in the preparation of Au/$ZrO_2$ nanocomposites.

## Results and discussion

Addition of a mixture of aqueous $Ce(NO_3)_3$ and $HAuCl_4$ to a solution of sodium alginate resulted in the formation of a gel through crosslinking of the polymer. On drying, the gel formed a clear, pink-purple film (Fig. 2a) indicating reduction of the $Au^{3+}$ precursor by alginate to form stabilized gold nanoparticles.

*School of Chemistry, University of Bristol, Bristol, UK BS81TS. E-mail: S.Mann@bristol.ac.uk*

† Electronic supplementary information (ESI) available: TEM of gold nanoparticles, EDXA of $CeO_2$ and Au, SAED of $CeO_2$ sponge and data for a control sample. See DOI: 10.1039/c0gc00338g

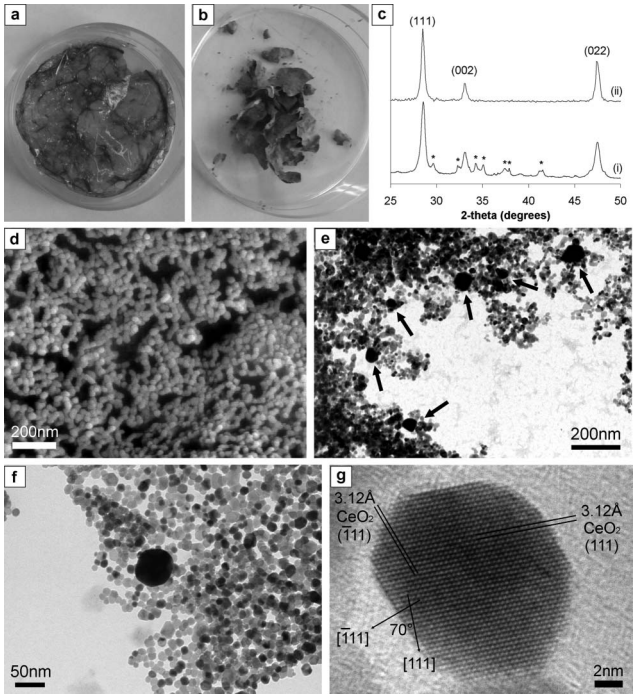


**Fig. 2** Optical images of (a) as-prepared alginate/Au/$Ce(NO_3)_3$ film and (b) corresponding Au/$CeO_2$ composite after calcination (theoretical Au mass of 5%). (c) PXRD profile of the sample (i) before and (ii) after washing in dilute HCl showing indexed peaks for $CeO_2$ and marked peaks for $Na_2CO_3$ (*). (d) SEM image of the Au/$CeO_2$ nanostructure. (e) TEM image of a typical Au/$CeO_2$ nanostructure (5% Au by weight) with arrows showing gold nanoparticles and (f) a single gold nanoparticle. (g) High resolution TEM of a single $CeO_2$ nanoparticle.

Transmission electron microscopy (TEM) of a sample redispersed in water confirmed the formation of gold nanoparticles (Fig. S1†). The colour of the film became more intense with increasing concentration of $HAuCl_4$ in the precursor solution (Fig. S2†). In a similar system, Pal *et al.*,[12] reported that the concentration of $HAuCl_4$ added to a sodium alginate solution did not affect the size of the resulting nanoparticles. Calcination of the dried film in air resulted in the formation of a light, delicate pink-purple solid (Fig. 2b). The colour of the composite again became more intense with increasing Au concentration (Fig. S2†). Powder X-ray diffraction (PXRD) indicated the primary phase to be cubic $CeO_2$ (*Fm3m*, ICDD 04-011-8938) with minor peaks corresponding to $Na_2CO_3$ (Fig. 2ci). This $Na_2CO_3$ phase, resulting from decomposition of the sodium alginate biopolymer could be simply removed by washing the sample in 0.1 M HCl, leaving a pure Au/$CeO_2$ sponge (Fig. 2cii). Nitrogen porosimetry indicated a specific surface area for the sample before and after washing of 4 $m^2\ g^{-1}$ and 31 $m^2\ g^{-1}$ respectively. Scanning and transmission electron microscopy (SEM, TEM) images of the sample showed a sponge-like structure of interconnected, monodisperse spherical $CeO_2$ particles (Fig. 2d–f), with a mean diameter of 20 nm ($\sigma$ = 25%). The sample containing 5 wt% Au showed discrete gold nanoparticles (diameter range 20–100 nm, mean 50 nm) dispersed through the reticulated structure. TEM images of the 1 wt% and 2 wt% Au samples showed Au nanoparticles of a similar size range, in agreement with the work of Pal *et al.* Energy dispersive X-ray analysis (EDXA) detected peaks for Ce in the bulk network and for Au in the darker gold nanoparticles (Fig. S3†). Corresponding selected area electron diffraction (SAED) displayed a series of rings characteristic of cubic $CeO_2$, confirming the crystalline nature of the nanoparticle sponge (Fig. S4†). Furthermore, high-resolution TEM of individual nanoparticles showed a regular pattern of fringes corresponding to the (111) and ($\bar{1}$1) set of planes and an interplanar angle characteristic of cubic $CeO_2$, indicating that each nanoparticle was a single crystal (Fig. 2g). A PXRD pattern of a control sample calcined in the absence of alginate also showed peaks characteristic of $CeO_2$ (Fig. S5b†). However, SEM and TEM images of the control showed a more densely packed structure with no evidence of a sponge-like network of nanoparticles (Fig. S5c,d†).

To investigate the mechanism of formation of the $CeO_2$/Au sponge, a series of samples were quenched at 100 °C intervals during calcination. PXRD patterns of the samples indicated that the onset of $CeO_2$ formation was between 300 °C and 400 °C and the broad peaks were consistent with the observation of nanoparticles (Fig. 3a). The Scherrer equation was used to estimate the mean $CeO_2$ particle size from XRD patterns for samples quenched at 50 °C intervals from 400 °C. These data showed a slight increase in the $CeO_2$ particle size during calcination (Fig. 3b), with the final particle diameter consistent with that observed by TEM.

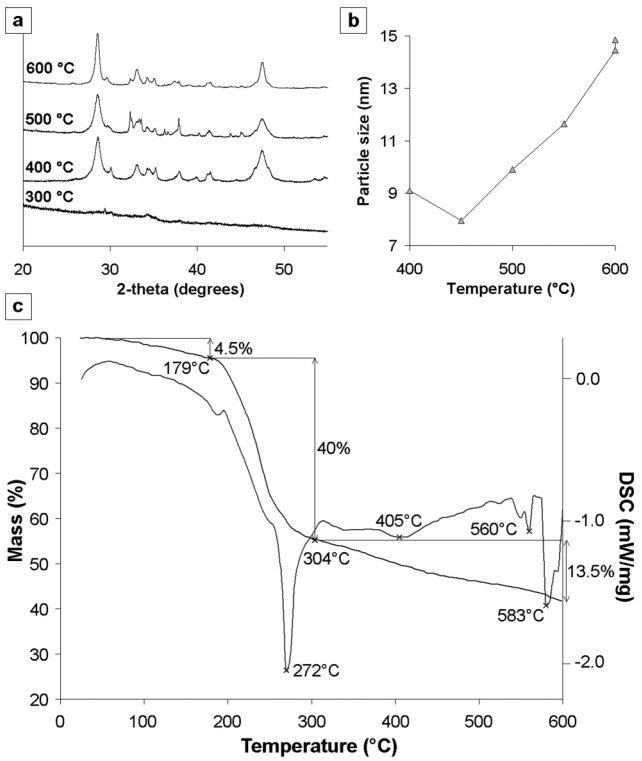


**Fig. 3** (a) PXRD profile of samples quenched at 100 °C intervals, (b) plot showing $CeO_2$ particle size with increasing temperature estimated using the Scherrer equation, and (c) TGA (left side upper plot) and DSC (left side lower plot) profiles.

Thermogravimetric analysis (TG) and differential scanning calorimetry (DSC) offered further insight into the mechanism

of $CeO_2$ nanoparticle formation (Fig. 3c). The initial mass loss of 4.5% was ascribed to the loss of bound water molecules. A second mass loss of 40%, between 180 °C and 300 °C with a strong exothermic peak at 272 °C, corresponded to the main decomposition step of the biological polymer. The group of exothermic peaks at 583 °C were possibly associated with the final decomposition stage of residual carbonaceous products. Although there are no previous studies of the decomposition of cerium alginate, the above TGA and DSC values were similar to those previously determined for a range of metal alginate compounds published by Said *et al.*[9]

Based on the observations described above, we propose that the alginate biopolymer has three key functions in the formation of the $Au/CeO_2$ nanocomposite. Firstly, the carboxylate-rich structure enables reduction of the $Au^{3+}$ precursor and stabilisation of the resulting gold nanoparticles. In the well-known citrate method, it has been suggested that the reduction of gold occurs *via* a process of oxidative decarboxylation with remaining carboxylate groups stabilizing the resulting gold nanoparticles and it seems likely that the mechanism of alginate reduction of gold proceeds *via* a similar route. Secondly, the biopolymer acts as a template for the nucleation of $CeO_2$. As mentioned above, alginate is known to strongly bind multi-valent cations through a mechanism known as the egg-box model.[13] By complexing and dispersing the $Ce^{3+}$ ions into microcrystalline regions within the gel, the initial nucleation of $CeO_2$ is constrained to nanoparticles. Finally, since metal-alginate compounds are known to be stable to relatively high temperatures, it is likely that the decomposition products of the polymer help to prevent significant mass-transport and sintering of these Au and $CeO_2$ nanoparticles before complete combustion of organic material to leave a porous $Au/CeO_2$ sponge.

To investigate the scope of this method, a gel was prepared from $ZrO(NO_3)_2$, $HAuCl_4$ and sodium alginate. On drying, the gel turned a pink-purple colour, which was retained on calcination to 600 °C. TEM images (Fig. 4a) showed Au nanoparticles (in the same size range as the $Au/CeO_2$ composites) dispersed in a matrix of $ZrO_2$ nanoparticles of mean diameter 9 nm. PXRD (Fig. 4b) showed peaks characteristic of $ZrO_2$ (ICDD 04-006-0278) and $Na_2CO_3$ which could be removed as before by washing with 0.1 M HCl. Nitrogen porosimetry indicated a surface area for the sample before and after washing of 3 $m^2\ g^{-1}$ and 47 $m^2\ g^{-1}$, respectively.

Finally, alternative biopolymer precursors were employed to study the effect on the structure of the $CeO_2$ and also to circumvent the formation of $Na_2CO_3$. Fig. 4 shows TEM images and PXRD patterns for samples of $CeO_2$ synthesized from (c,d) agar and (e,f) ammonium alginate. Agar produced a gel-like network with a surface area of 13 $m^2\ g^{-1}$. Ammonium alginate generated clustered nanoparticles of mean diameter 11 nm and surface area of 10 $m^2\ g^{-1}$. The use of the sodium-free biopolymers eliminated the sodium carbonate byproduct and so may offer a route to optimise the synthesis and structure of metal/metal oxide composites *via* this simple method.

## Conclusions

In summary, we have demonstrated a remarkably simple, one-pot route to the synthesis of a nanoparticulate $Au/CeO_2$ sponge using a readily available biopolymer alginate template. The multi-functionality of the alginate biopolymer in reducing the $Au^{3+}$ precursor and controlling and stabilising $CeO_2$ nucleation has been discussed. Furthermore, the potential scope of the method has been demonstrated through the synthesis of an $Au/ZrO_2$ nanocomposite. This simple and flexible approach offers considerable potential for future development in the synthesis of metal/metal oxide composites. There are numerous examples in the literature of metal nanoparticles, such as Au, Pt, Ru, Rh, Pd and Ag, supported on porous metal oxide supports (*e.g.* $ZrO_2$, CuO, ZnO) and our biopolymer-mediated, one-pot route should offer significant advantages over many previous synthesis techniques.

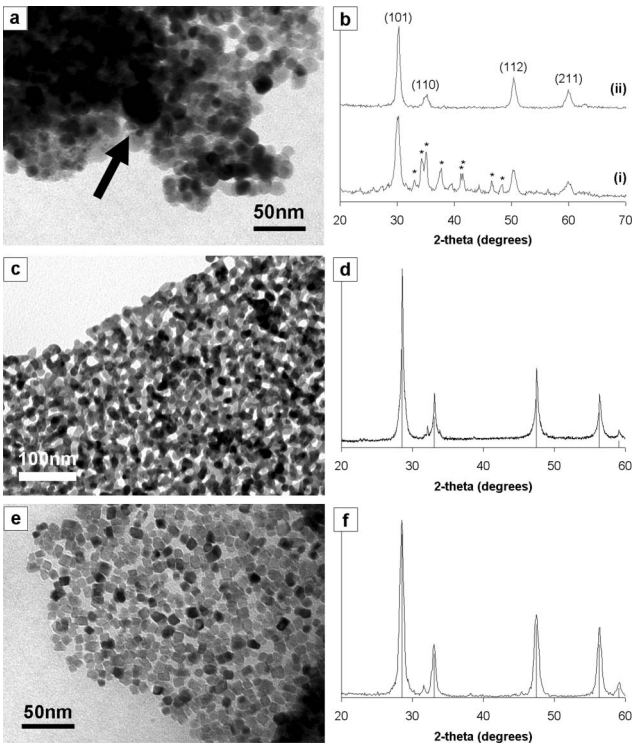


**Fig. 4** (a) TEM image of an $Au/ZrO_2$ composite synthesized from alginate. (b) PXRD profile of the sample (i) before and (ii) after washing in dilute HCl showing indexed peaks for $ZrO_2$ and marked peaks for $Na_2CO_3$ (*). (c) TEM image and (d) PXRD pattern for $CeO_2$ synthesized from agar and (e) TEM image and (f) PXRD pattern for $CeO_2$ synthesized from ammonium alginate.

## Experimental

Biopolymer solutions were prepared at 80 °C from 0.1 g of sodium alginate (FMC Biopolymer, LF20/40, 65–75% guluronate) in 10 mL of deionised water. Gels were prepared by premixing 2 mL of a solution of $Ce(NO_3)_3$ (20 mM in deionised water) with a solution of $HAuCl_4$ (at a range of concentrations in deionised water) and vigorously mixing the resulting solution with the alginate solution. The desired concentration of gold was calculated assuming complete conversion of $4 \times 10^{-5}$ moles of $Ce(NO_3)_3$ to $CeO_2$. Thus, a 1% by mass Au on $CeO_2$ composite was prepared using 0.018 mL of aqueous $HAuCl_4$ (20 mM), 2% from 0.035 mL and 5% from 0.088 mL. The gel was dried at room temperature for 48 h to form a flexible pink or purple film

 

that was calcined in air at 1 °C $min^{-1}$ to 600 °C for two hours. Control syntheses in the absence of sodium alginate were also carried out. $ZrO_2$/Au nanocomposites were prepared in the same way using aqueous $ZrO(NO_3)_2$ (0.02 M). Agar solution (1% by weight) was prepared by dissolving agar (Aldrich) in boiling water. Ammonium alginate was prepared by stirring alginic acid (FMC Biopolymer) in water and adjusting the pH to 7 with ammonium hydroxide.

Samples for TEM were prepared by dispersing in ethanol and dropping onto a carbon coated nickel grid. TEM analysis was carried out using a JEOL JEM 1200EX microscope equipped with an Oxford EDX detector and high resolution TEM carried out on a JEOL JEM 2010 microscope. Samples for SEM were coated with platinum/palladium and analysed using a JEOL JSM 6330F Field Emission SEM. PXRD was carried out on a Bruker D8 Advance diffractometer equipped with a Lynxeye position sensitive detector.

## Acknowledgements

The authors thank the University of Bristol for financial support and FMC Biopolymer for samples of alginate. We are grateful to Prof. G. Hutchings and Dr P. Miedziak for useful discussion.

## Notes and references

1 R. J. White, R. Luque, V. L. Budarin, J. H. Clark and D. J. Macquarrie, *Chem. Soc. Rev.*, 2009, **38**, 481–494.
2 J. Beckers and G. Rothernberg, *Green Chem.*, 2010, **12**, 939–948.
3 X. Wang, D. R. G. Mitchell, K. Prince, A. J. Atanacio and R. A. Caruso, *Chem. Mater.*, 2008, **20**, 3917–3926.
4 O. Rosseler, M. V. Shankar, M. Karkmaz-Le Du, L. Schmidlin, N. Keller and V. Keller, *J. Catal.*, 2010, **269**, 179–190.
5 M. Sahnchez-Dominguez, L. F. Liotta, G. Di Carlo, G. Pantaleo, A. M. Venezia, C. Solans and M. Boutonnet, *Catal. Today*, 2010, **158**, 35–43.
6 R. Si and M. Flytzani-Stephanopoulos, *Angew. Chem., Int. Ed.*, 2005, **44**, 7411–7414.
7 Z. Schnepp, S. C. Wimbush, S. Mann and S. R. Hall, *CrystEngComm*, 2010, **12**, 1410–1415.
8 J. M. Nieto and C. Peniche-Covas, *Thermochim. Acta*, 1991, **176**, 63–68.
9 A. A. Said and R. M. Hassan, *Polym. Degrad. Stab.*, 1993, **39**, 393–397.
10 M. Cargnello, C. Gentilini, T. Montini, E. Fonda, S. Mehraeen, M. Chi, M. Herrera-Collado, N. D. Browning, S. Polizzi, L. Pasquato and P. Fornasiero, *Chem. Mater.*, 2010, **22**, 4335–4345.
11 S. Carrettin, P. Concepcion, A. Corma, J. M. Lopez Nieto and V. F. Puntes, *Angew. Chem., Int. Ed.*, 2004, **43**, 2538–2450.
12 A. Pal, K. Esumi and T. Pal, *J. Colloid Interface Sci.*, 2005, **288**, 396–401.
13 G. T. Grant, E. R. Morris, D. A. Rees, P. J. C. Smith and D. Thom, *FEBS Lett.*, 1973, **32**, 195–198.